Development of an injury risk function for a HBM with a specific fracture in the lower extremities

Christoph Klein, Katarina Kljajić, Oliver Zehbe, Stefan Kirschbichler, Werner Leitgeb

Abstract Accurate assessment of lower extremity injuries is crucial for mitigating long term personal and socio-economic consequences of traffic accidents. Due to the frequent occurrence of injuries in the ankle complex, an injury risk function for the prediction of calcaneus fractures was developed and a Finite Element (FE) model of a THUMS v4 M50 lower leg was improved. A study with sixty pendulum impacts on post-mortem human subjects (PMHS), conducted in neutral and dorsiflexed foot positions, was selected. Improvements to the Human Body Model (HBM) were done to reproduce the force/compression characteristics reported in the PMHS study.

The improved model was used to replicate the PMHS tests, with impact energy scaled to specimen height. Forces and strains were extracted at multiple anatomical locations, and injury risk functions were derived by correlating simulation outputs with fracture outcomes from the PMHS study. Brier Metric Scores were computed to identify the most effective predictor for the injury. Among all evaluated metrics, calcaneus strain showed the highest predictive capability for fracture occurrence. The study provides a calcaneus specific injury risk function (IRF) for THUMS v4 50M, advancing prediction of lower limb injuries with potential long-term consequences.

Keywords Injury risk function, Calcaneus fractures, Lower limb injuries

INTRODUCTION

Efforts to reduce the consequences of road traffic accidents have traditionally focused on preventing fatal injuries. However, the assessment methods and statistical indicators used to evaluate these injuries do not sufficiently account for the long-term consequences of crashes [1]. These consequences also cannot be derived from the established Maximum Abbreviated Injury Scale (MAIS), as some injuries with low MAIS can lead to long-term consequences and additionally some injuries with higher MAIS have a lower risk for long-term consequences [2]. Therefore, injury risk criteria that specifically address injuries which result in a higher risk for long-term consequences are needed.

Injuries in the lower extremities are associated with long term consequences for the patients. This includes a reduction in the quality of life [3] and the inability to work, with lower extremity injuries representing the leading cause of work incapacity [4]. Furthermore, studies [5, 6] indicate that the lower extremities are among the top three body regions most frequently linked to long-term consequences when injured. Among the injuries in the lower extremities, those in the ankle complex are the most common ones [7], with a share of calcaneus fractures of 15 – 32 % for lower extremity injuries [8]. Injury risk functions for the lower extremities are available in literature [9], but they often represent the risk of the specimen under a certain load in the test to be injured, and do not consider the loads on a certain virtual model in a simulation.

The present study aims to contribute to the mitigation of injuries with long-term consequences, by developing an injury risk function (IRF) for the prediction of calcaneus fractures and improving a model in the ankle complex. The IRF is developed for a THUMS v4 M50 with underlying PMHS experimental data reported in literature.

C. Klein (+43 316 873 9624, christoph.klein@v2c2.at), K. Kljajic, O. Zehbe, S. Kirschbichler and W. Leitgeb are researchers at Virtual Vehicle Research GmbH in Graz, Austria.

METHODS

For the development of an injury risk function, an existing PMHS dataset from literature was utilized. Initially, an off the shelf HBM was identified based on pre-defined criteria. The force/compression behaviour in the ankle complex of the HBM was improved for selected cases of a PMHS study. Next, the entire PMHS study was reproduced by simulating an improved HBM. Based on the simulation data and the documented injuries from the study, an IRF was derived.

PMHS data selection

Publicly available datasets from existing PMHS studies, as outlined in Table 1 were considered for the development of the IRF. From these, a dataset was selected, according to the following criteria:

Unbooted specimen: In case booted specimens were used, a validated model of the boot would also be required.

Detailed information about the specimen's anthropometry and about the test setup was available: To virtually replicate the test setup, a detailed description is necessary. Anthropometrical information is needed to either scale the impact energy or morph the FE model to the specimen's geometry.

For the development of the IRF, injured and uninjured specimen test results should be balanced in the study.

Table 1: PMHS studies

Author / Year	Number of specimens	Overview / additional information	Injuries (case numbers)
Kitagawa 1998 [10]	16	Pendulum	Pylon FX (5) Calcaneal FX (10)
Gallenberger 2009 [11, 12]	15	60 pendulum impacts (thereof 19 in 20 deg dorsiflexion)	Calcaneal FX (17), Tibia FX(2)
Funk 2000 [13]	92	Compression on sled, Specimen information missing	Calcaneal FX (23), Malleolar FX (11), Talar FX (10), Fibula FX (4), Several injuries (11)
Klopp 1997 [14]	50	Compression on sled, detailed description of the test setup missing	Calcaneal FX, Talus FX, Malleoli FX

From the aforementioned PMHS studies, those by Funk and Klopp were excluded from further consideration due to insufficient details regarding either test setup or specimen. Additionally, the data reported by Kitagawa were not utilized, as the injured specimen were classified as left-censored and only a single test with an uninjured specimen is reported. The dataset from Gallenberger fulfilled the defined criteria and was therefore selected for this study.

PMHS test cases

A total of 60 pendulum impacts on the plantar surface of 15 specimens were performed by [11, 12]. Of these, 19 impacts were applied to specimen positioned in 20 deg in dorsiflexion. Pendulums with masses of 3.3 kg, 5.7 kg and 12.3 kg were used to impact the lower limb (see Fig. 1). The proximal end of the lower limb was potted, and an additional ballast mass was added to achieve a total weight of 11.5 kg including foot, potting, load cell and ballast. Impact velocities ranged from 2 to 9 m/s. Foot-ankle response (compression and force on the ballast mass) were analysed for different impact velocities and resulting injuries (mostly calcaneus fractures) were documented.

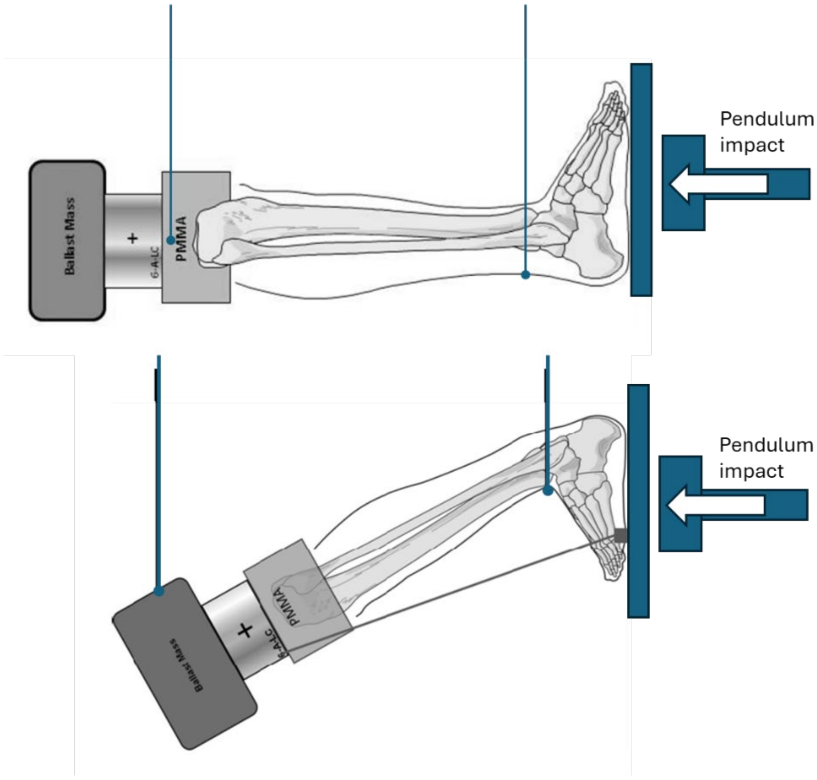

Fig. 1: PMHS pendulum tests in neutral and in dorsiflexion position [11, 12]

For each specimen the tests started with a lower impact energy and was increased with each test until an injury occurred. The reported injuries were calcaneus fractures for all cases except one. The impact velocities, the pendulum mass and the basic anthropometric information for each specimen were documented.

Selection of a FE HBM lower limb

The lower limb of an FE HBM was selected among royalty free models and according to the following criteria:

The ankle complex needs to be modelled with smooth surfaces: Coarse elements could lead to high inner artificial loads and further an overprediction of injury risk

Deformable material models were used: Forces and strains were considered as predictors. For the strain calculation, deformable material is required.

The joints in the ankle complex were modelled as contact-based joints: In case of deformable materials, kinematic joints could be attached to the bone by using rigid patches. That would also introduce local artificial loads on the bones.

The considered HBMs for the selection were a THUMS v3, THUMS v4 and a Viva+ model. The average for height and weight of the specimens were 1.77 m and 82 kg. Therefore, the 50M version of the models was considered. Among the listed models, Viva+ was not further considered due to the kinematic joint modelling and THUMSv3 due to the element size and unrefined and coarse geometry details in the ankle complex. Consequently, THUMS v4 M50 was selected and the lower limb model was isolated for usage in this study. Material failure and element erosion is not depicted in the model.

FE HBM improvements

For the FE simulation, the HBM was cut off at the proximal surface of the tibia. All distal parts and contacts were preserved from the original model. A potting was added at the proximal end of the tibia. An additional mass was added on a node at the end of the potting, which depicts the ballast mass. Further, a mass was added to the pendulum plate to represent the pendulum mass. The fixation of the specimen with cables was depicted by adding kinematic boundary conditions in the FE model. (See Fig. 1 and Fig. 2)

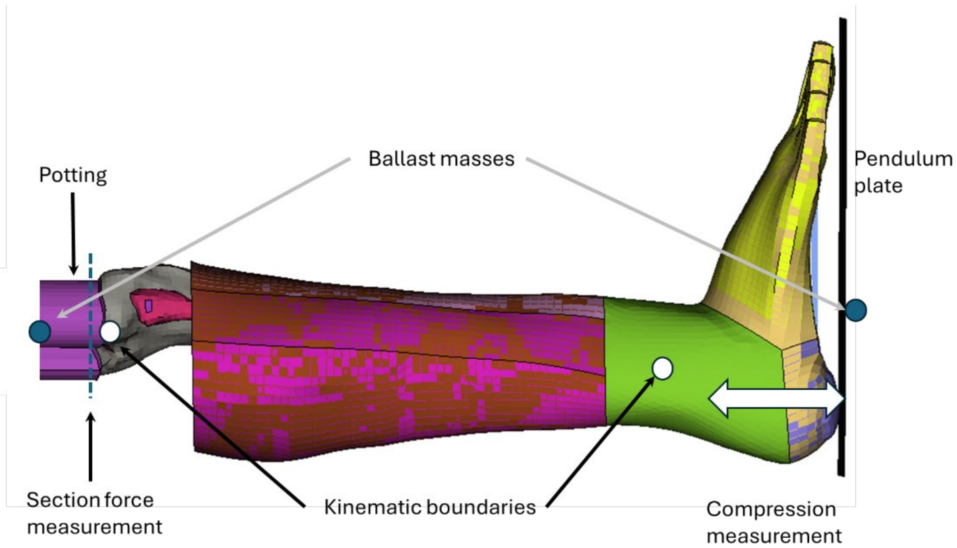

Fig. 2: Boundaries of the PMHS study depicted with the FE HBM lower leg

To check the biofidelity of the model in the ankle complex, section force and the compression of the foot relative to the pendulum plate were measured during the simulation and compared to the results of four identified cases of the PMHS study (see Fig. 2). The criteria for case selection were, that the range of impact energy (6J to 237J) is represented, and that test results (compression and forces) are documented. As shown in Table 2, the four selected cases had an energy of 40 J, 60 J, 130 J and 237 J. Detailed information are given in Table 5 and Table 6 in the Appendix.

Table 2: Impact boundaries

Test Nr.	Pendulum mass [kg]	Impact velocity [m/s]	Impact energy [J]
PCLE 249	3.36	4.88	39.95
PCLE 251	5.76	4.65	62.26
PCLE 254	5.76	9.09	237.9
PCLE 259	3.36	8.95	134.6

Simulating the off the shelf version of the HBM lower leg showed differences in compression and force compared to the PMHS study (see Table 3 in the results section). Similar issues and required adjustments are reported by [15, 16], which enhanced THUMS v4.1 small female model and a THUMS v6.1 50^{th} percentile male model. The following refinements were made to the lower limb FE model for this study (Fig. 3).

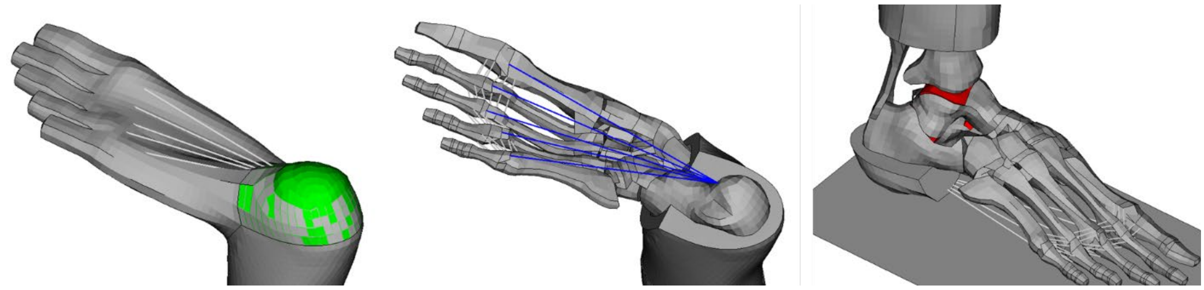

Fig. 3: Refinements for the lower limb: Heel tissue, planta fascia and cartilage

Plantar Fascia

The dynamics of the foot with a longitudinal loading is influenced by the plantar fascia, which was missing in the THUMS v4 M50. It was modelled using five 1D beam elements between the calcaneus and the metatarsal bones. The beam was modelled with a Mat Elastic material and the properties were adjusted as suggested in [17] and further adapted in the improvement process, which resulted in a Young's modulus of 150 kPa.

Heel tissue

The heel flesh thickness below the calcaneus is approximately 6 mm in the THUMS v4 M50. Ref. [18] showed that the heel tissue below the calcaneus is between 10 and 15 mm for people with the same height as the THUMS v4 50M. Accordingly a conforming heel pad with a maximum thickness of 4 mm was added. Material property adaption was initialized with the material values of the heel flesh and let to a bulk modulus of 125 kPa for the additional heel tissue. This additional flesh mainly influences the force/compression characteristics in the first part of the loading phase.

Cartilage between Talus, Tibia and Calcaneus

To avoid a direct bone-to-bone contact in the ankle complex, and soften the contact characteristics, additional cartilage was added between the talus, tibia and the calcaneus as suggested in [19].

FE Simulation of the PMHS test series

The 60 cases of the PMHS study were simulated with the improved FE lower leg model. As the HBM lower leg and each individual specimen differ in terms of anthropometry, either the HBM needs to be morphed to the specimen's geometry, or the boundaries of the pendulum impact need to be adjusted for the FE simulation accordingly. In this study, the energy of the impact in the simulations was scaled to the anthropometry of the specimen and the HBM was not morphed, since anthropometrical information about the ankle complex was not documented in the PMHS study. The proportions of the ankle region correlate with the height of a person [20]. Therefore, the kinematic energy of the pendulum in each test was scaled according to the ratio of the specimen height to the HBM height. Subsequently, the pendulum velocity for the simulation was calculated from the scaled kinematic energy. Table 5 in the Appendix shows the anthropometrical information of each specimen as well as the documented boundaries of the impact test and the modified boundaries for the simulation.

For the development of the injury risk function, section forces and the maximum value of the 99 percentile of the principal strains (PS99) were determined for the upper tibia, mid tibia, lower tibia, talus and calcaneus as shown in Fig. 4. This follows the approach presented in [21].

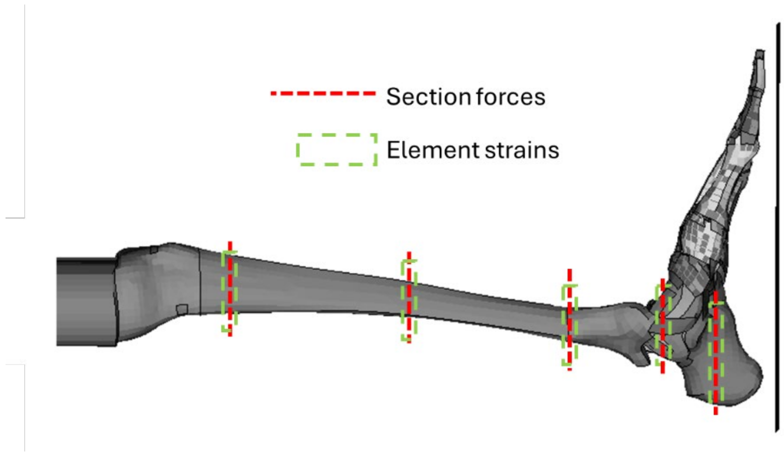

Fig. 4: Measurement locations in the simulation model

Development of the Injury Risk Function

The impact energy for each specimen was increased during the test series until injuries occurred. The injuries were mostly fractures of the calcaneus. As the injury risk function in this study was developed specifically for calcaneus, all other injuries were treated as uninjured for the IRF development. Table 6 in the Appendix shows the injuries for each of the 60 PMHS tests, the impact energy and the corresponding censor.

The uninjured test runs were defined as right-censored, whereas the injured were taken as left-censored. These data of the PMHS test series are used in combination with the measurements of the simulation study to develop IRF for each of the measured simulation outputs (forces, strains). The post-processing tool Dynasaur [22] was used to extract the PS99 strain for the defined measurement regions. For each of the regions, an IRF based on a Weibull function was defined. Parameter estimation for the function was done with the Python package Lifelines [23]. To determine which of the IRF is the best predictor for calcaneus fractures, the Brier Metric Score (BMS) [24] was calculated for each of the IRFs.

RESULTS

Improved ankle region for THUMS v4 M50

Adaptions were made by adding a plantar fascia, heel tissue and cartilage between the bones as explained in the methods section. Table 3 shows the forces and compressions of the simulation in comparison to the PMHS study with the original THUMS setting (left) and with the refinements (right) for the selected four cases as described in the methods section. The four cases were selected to consider the range of impact energy in the test series. As for the different energy levels, detailed information is not available for all specimen, specimen responses corridors were not calculated.

Table 3: Compression and forces for the original and the improved THUMS v4 M50 lower leg

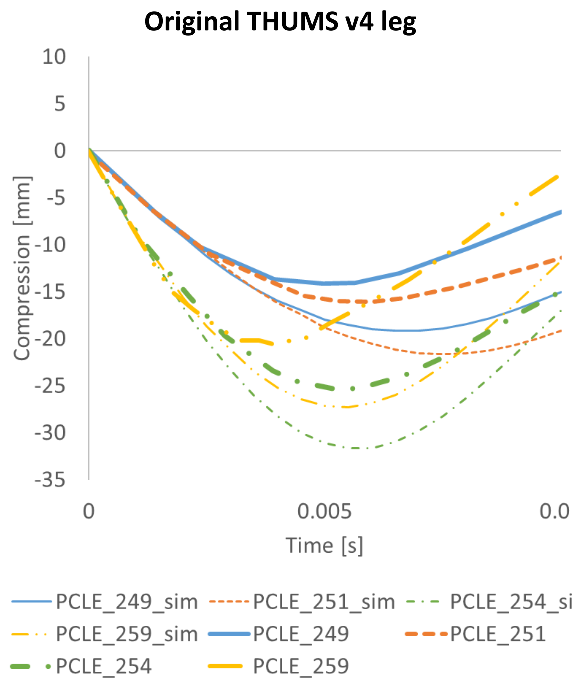

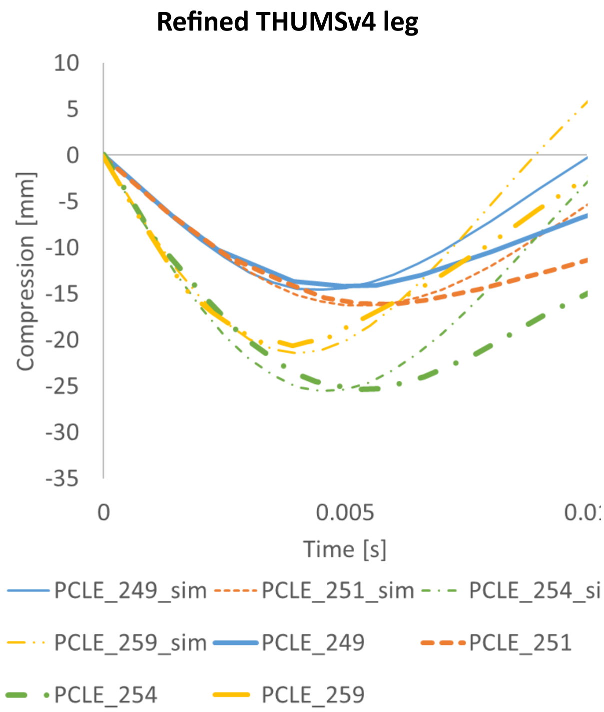

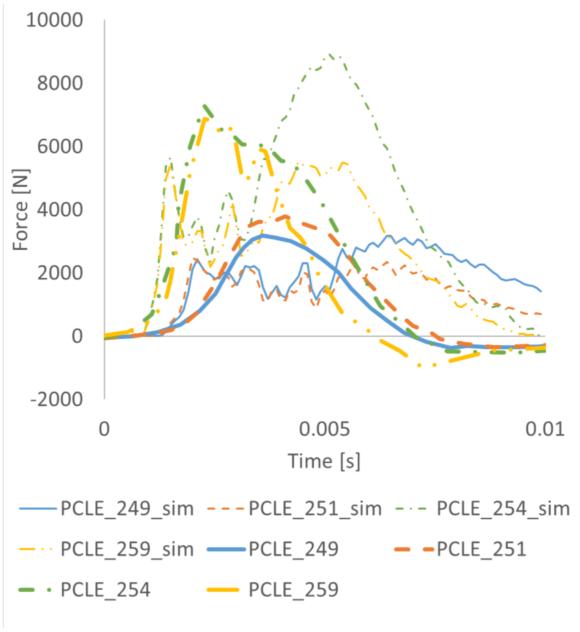

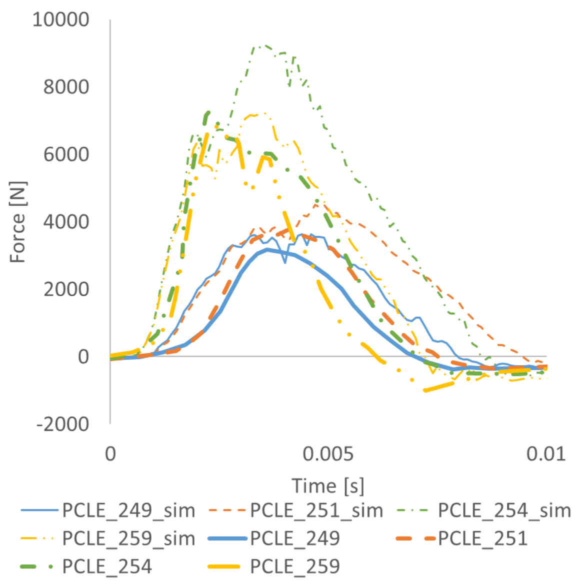

Due to the refinements in the ankle complex, the compression became more biofidelic in terms of maximum compression and the loading phase of the motion. The unloading phase of the motion shows differences, but the focus in this study is on the loading phase and the maximum compression where the fracture occurs. For the forces, the model was improved with respect to the loading phase in terms of timing and gradient of the force. Further, the overall characteristics in terms of timing and shape were enhanced for all cases. The maximum force level is represented properly for the three cases which do not report a fracture of the calcaneus. Following table shows the CORA rating for the original and the improved version of the ankle complex.

Table 4: CORA Rating

	Compression		Force	
Test Number	Original	Improved	Original	Improved
PCLE 249	0.67	0.81	0.31	0.86
PCLE 251	0.74	0.86	0.52	0.83
PCLE 254	0.78	0.78	0.50	0.85
PCLE 259	0.66	0.88	0.46	0.85

Injury risk function

For each of the force and strain measurements in the simulation model (upper, mid and lower tibia, talus, calcaneus), IRF were defined, as described in the method section. Subsequently, the BMS (see Fig. 5) was calculated to identify the best predictor for calcaneus fractures.

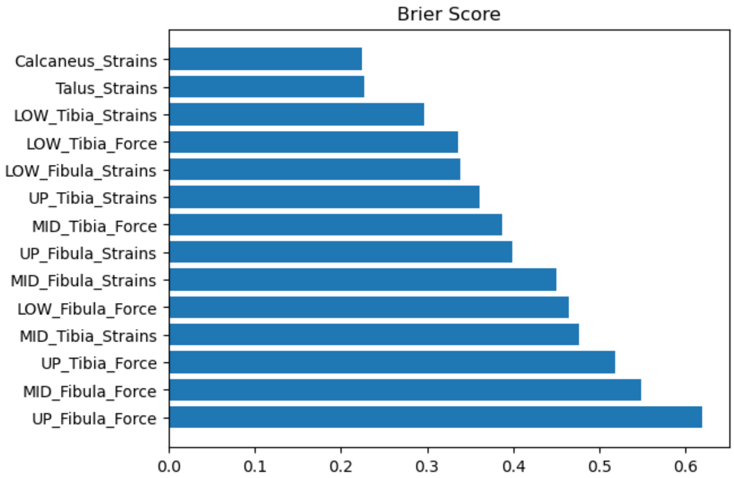

Fig. 5: Brier Metric Score

The lowest BMS value indicates the function with the highest prediction quality. Hence, the maximum value of the 99th percentile of the measured calcaneus strains is the best predictor for calcaneus fractures. The following formula (1) allows to calculate the injury risk based on the calcaneus strains:

$$\text{Injury risk} = 1 - e^{\left(\frac{\max PS99\ strain}{0.0316}\right)^{2.5998}} \qquad (1)$$

Fig. 6 shows the injury risk function of the element strains and additionally the injury status of the PMHS tests with the respective strains for those cases from the simulation model.

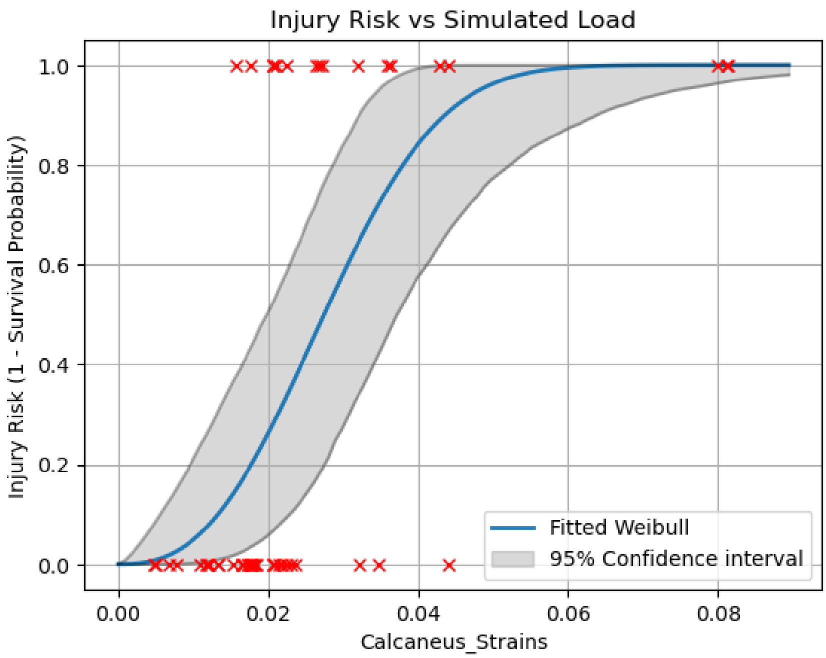

Fig. 6: Injury risk function for calcaneus fractures and injury status of the PMHS tests with the corresponding load in the simulation study

DISCUSSION

In this study, an injury risk function for the prediction of calcaneus fractures and an improved model of the ankle complex for a THUMS v4 M50 was developed. Among existing HBMs, the THUMS v4 M50 was identified based on pre-defined criteria. Additionally, a PMHS dataset from a pendulum impact test was selected from literature. Four runs of the PMHS study with different impact energies were chosen for model validation as an initial step. The HBM was adapted in the ankle region and simulation results were compared to the test data with respect to force and compression. Since fractures typically occur either during the loading phase or at the point of maximum load, the assessment of model biofidelity focused on the loading phase while the specimens remained uninjured. Due to model refinement, the compression behavior and resulting forces could be aligned with the PMHS data. With the model improvements, the complete PMHS study was simulated. Simulation results (forces, strains) and injury information from the PMHS study were then combined, and an injury risk function for the prediction of calcaneus fractures was developed.

Limitations of the study:

Age Dependency

The developed IRF is independent from age. The reason for not including age as a parameter is that it would lead to results, in which the predicted risk for a calcaneus fracture decreases with increasing age. This effect arises from the age distribution of the specimens and the energy levels at which injuries occurred in this specific PMHS study (see Table 6 in the Appendix). Fig. 7 shows energy level over age for the tests which led to injuries. The regression line in the diagram indicates that specimens with a higher age appear more likely to withstand higher loads. As this stands in contrast to other age-dependent IRF [25, 26], age was not considered in the development of the IRF in this study.

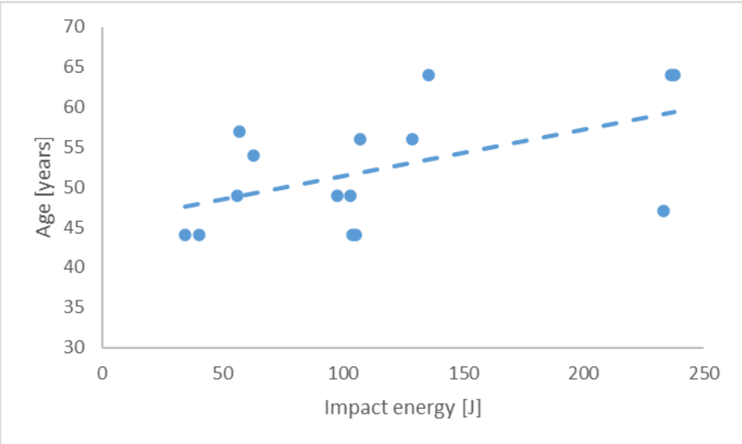

Fig. 7: Age over impact energy for tests in which calcaneus fractures occurred in the PMHS study

Modelling of the plantar fascia

One of the refinements for the HBM was the plantar fascia, which was added to the existing THUMSv4 M50. It was modelled with five 1D beam elements using a MAT Elastic material model. For further improvement, this structure could be modelled with 2D or 3D elements, using more biofidelic geometry and material modelling.

PMHS data from literature

As detailed geometrical information about each specimen was not available, morphing the FE model to the individual geometry was not possible. Therefore, the assumption was made, that loading each specimen in the simulation study with a scaled impact energy depicts the PMHS test. Individualization is done by scaling the impact energy according to the height ratio of the HBM and the specimen. Based on that, the impact velocity was determined.

CONCLUSION

Injuries in the lower extremities lead to long-term consequences for individuals and at the socio-economic level. Among the injuries in the lower extremities, ankle fractures are the most common type of injury. This study aimed to develop an injury risk function for calcaneus fractures and an improved ankle complex for an existing HBM. Requirements for the HBM were defined and accordingly the THUMS v4 M50 was selected for this study. Further, a PMHS study from literature was selected based on defined requirements for the PMHS data set. Improvements in the HBMs ankle complex were made, based on four cases from the PMHS study with different energy levels. During this process, a plantar fascia, heel flesh and cartilage between tibia, calcaneus and talus were added to the model. With the validated model, the PMHS study was reproduced by simulation (60 cases, including 19 in dorsiflexion). Loads were measured in the simulation at various anatomical locations in the lower limb. For these measurements, the parameters of a Weibull based IRF were defined. The BMS was calculated to identify principal strains in calcaneus as the best predictor for calcaneus fractures. With that, it is possible to predict calcaneus fractures with the THUMS v4 M50 and thereby contribute to reducing injuries which potentially lead to long term consequences.

ACKNOWLEDGEMENT

The work described was carried out as part of the project ProtAct-Us (Grant No. 101147445).

The project is funded by the European Union. Views and opinions expressed are however those of the author(s) only and do not necessarily reflect those of the European Union or European Climate, Infrastructure and Environment Executive Agency (CINEA). Neither the European Union nor the granting authority can be held responsible for them.

The publication was written at Virtual Vehicle Research GmbH in Graz and partially funded within the COMET K2 Competence Centers for Excellent Technologies by the Austrian Federal Ministry for Innovation, Mobility and Infrastructure (BMIMI), Austrian Federal Ministry for Economy, Energy and Tourism (BMWET), the Province of Styria (Dept. 12) and the Styrian Business Promotion Agency (SFG). The Austrian Research Promotion Agency (FFG) has been authorised for the programme management.

LITERATURE

[1] European Commission (2023) Road Safety Thematic Report – Consequences of crashes. European Road Safety Observatory. Brussels, European Commission, Directorate General for Transport.

[2] Stigson, H., Boström, M. & Kullgren, A (2020). Health status and quality of life among road users with permanent medical impairment several years after the crash. Traffic Inj Prev.

[3] Barnes J., Thomas Pete, Quality of Life Outcomes in a hospitalized sample of road users involved in crashes, https://pmc.ncbi.nlm.nih.gov/articles/PMC3217474/pdf/aam50_p239.pdf [26.03.2026]

[4] Johannsen H., Long Term Consequences of Road Accidents, https://bast.opus.hbz-nrw.de/frontdoor/deliver/index/docId/1811/file/F117_31.pdf [26.03.2026]

[5] Jänsch M. et al., (2025) Identification of accident scenarios with a special relevance for injuries and psychological impairments that result in long-term consequences, *Proceedings of the IRCOBI conference 2025*, Vilnius

[6] Kullgren A. et al., (2020) Development in car crash safety since the 1980s, *Proceedings of the IRCOBI conference 2020,* online Conference

[7] Forman J. et al., (2019) Automobile injury trends in the contemporary fleet: Belted occupants in frontal collisions, Traffic Injury Prevention, 20:6, 607-612, DOI: 10.1080/15389588.2019.1630825

[8] Benson E. et al., (2007) Calcaneal fractures in occupants involved in severe frontal motor vehicle crashes, Accident Analysis and Prevention 39, p. 794 – 799.

[9] Rupp J.D. et al., (2009) Development of New Injury Risk curves for the Knee/disal femur and the hip for use in frontal impact testing, UMTRI Report No. UMTRI-2009-08

[10] Kitagawa Y. et al. (1998), A severe Ankle and Foot injury in Frontal Crashes and Its Mechanism, 42nd Stapp Car Crash Conference Proceedings, Paper Nr. 983145

[11] Gallenberger K., (2009), Biomechanics of Foot and Ankle Injuries In Variable Energy Impacts Master's Theses

[12] Gallenberger K., (2013), Biomechanics of foot/ankle trauma with variable energy Impacts, Annals of Advances in Automotive Medicine, 57th AAAM Conference

[13] Funk J.R., (2002), The Axial Injury Tolerance of the Human Foot/Ankle Complex and the Effect of Achilles Tension. Journal of BiomechEng 124(6): 750-757

[14] Klopp G.S., et al. (1997), Mechanisms of Injury and Injury Criteria for the Human Foot and Ankle in Dynamic Axial Impacts to the Foot, *Proceedings of the IRCOBI conference*, Hannover

[15] Iyer R.B. et al., (2024), Refinement and Biofidelity Evaluation of the THUMS Small Female Ankle, *Proceedings of the IRCOBI conference 2024*

[16] Iyer R.B. et al., (2025), Enhancing Biofidelity of THUMS 50th Percentila Male Foot and Ankle: Refinements and Validations, *Proceedings of the IRCOBI conference 2025*

[17] Qian Z, et al. (2021), Morphology and Mechanical Properties of Plantar Fascia in Flexible Flatfoot: A Noninvasive In Vivo Study., Front. Bioeng. Biotechnol. 9:727940. doi: 10.3389/fbioe.2021.727940

[18] Toshihiro Maemichi, et al., (2020) The relationship of heel fat pad thickness with age and physiques in Japanese, Clinical Biomechanics, Volume 80

[19] Iyer R.B. et al., (2024) Refinement and Biofidelity Evaluation of the THUMS Small Female Ankle, *Proceedings of the IRCOBI conference,* Stockholm

[20] Astolfi R.S. et al., (2020) Foot structures and their correlations with body height, Forensic Science International: Reports, Volume 2

[21] Hostetler Z.S., Gayzick F.S., (2024), Lower Extremity Injury Risk Curve Development for a Human Body Model in the Underbody Blast Environment, ASME Journal of Biomechanical Engineering, Vol. 146

[22] https://gitlab.com/VSI-TUGraz/Dynasaur [26.03.2026]

[23] https://lifelines.readthedocs.io/en/latest/ [26.03.2026]

[24] Brier, G.W. (1950) Verification of Forecasts Expressed in Terms of Probability. Monthly Weather Review, 78, 1-3.

[25] Ridella et al., (2012), Age-Related Differences in AIS 3+ Crash Injury Risk, Types, Causation and Mechanisms, *Proceedings of the IRCOBI conference*, Dublin

[26] von Kleeck BW, et al., (2022) Age targeted human body models indicate increased thoracic injury risk with aging, Traffic Inj Prev. 2022

APPENDIX

Table 5: Scaled velocities and identified cases for model improvement (highlighted grey)

Test Number	Pendulum Mass (kg)	Impact Velocity (m/s)	Impact Energy (J)	Height (m)	Height THUMS v4	Height scaled energy	Height scaled velocity
PCLE200	3,3	2,02	6,76	1,78	1,786	6,78	**2,03**
PCLE201	3,3	3,99	26,22			26,31	**3,99**
PCLE202	5,7	3,04	26,4			26,49	**3,05**
PCLE203	5,7	4,02	46,14			46,30	**4,03**
PCLE204	5,7	5,95	100,75			101,09	**5,96**
PCLE205	3,3	7,71	97,96			98,29	**7,72**
PCLE206	5,7	9,05	233,22			234,01	**9,06**
PCLE207	3,3	2,07	7,07	1,78		7,09	**2,07**
PCLE215	3,3	3,99	26,31	1,7		26,40	**4,00**
PCLE216	3,3	5,83	56,06			56,25	**5,84**
PCLE217	12,32	3,18	62,28			62,49	**3,19**
PCLE218	12,32	4,17	107,12			107,48	**4,18**
PCLE219	3,3	8,84	128,85			129,28	**8,85**
PCLE227	3,3	4,95	40,43	1,57		40,57	**4,96**
PCLE228	3,3	7,94	104,02			104,37	**7,95**
PCLE229	3,3	4,56	34,31	1,57		34,43	**4,57**
PCLE230	3,3	7,99	105,34			105,70	**8,00**
PCLE249	3,36	4,88	39,95	1,73		40,08	**4,88**
PCLE250	3,36	5,67	53,99			54,17	**5,68**
PCLE251	5,76	4,65	62,26			62,47	**4,66**
PCLE252	3,36	4,88	39,94			40,07	**4,88**
PCLE253	3,36	8,99	135,72			136,18	**9,00**
PCLE254	5,76	9,09	237,89			238,69	**9,10**
PCLE255	3,36	4,93	40,78	1,73		40,92	**4,94**
PCLE256	3,36	6,01	60,58			60,78	**6,02**
PCLE257	5,76	4,43	56,54			56,73	**4,44**
PCLE258	3,36	4,94	41			41,14	**4,95**
PCLE259	3,36	8,95	134,59			135,04	**8,97**
PCLE260	3,36	4,98	41,71			41,85	**4,99**
PCLE261	5,76	9,06	236,31			237,11	**9,07**
PCLE262	3,36	4,95	41,08	1,75		41,22	**4,95**
PCLE263	3,36	5,75	55,47			55,66	**5,76**
PCLE264	5,76	4,67	62,84			63,05	**4,68**
PCLE265	3,36	4,94	40,93			41,07	**4,94**
PCLE266	3,36	4,97	41,45	1,8		41,59	**4,98**
PCLE267	3,36	5,93	59,24			59,44	**5,95**
PCLE268	5,76	4,45	57,05			57,24	**4,46**
WCOIOIAO 01	12,32	3,2	63,05	1,83		63,26	**3,20**
WCOIOIAO 02	12,32	4,09	103,05			103,40	**4,10**
WCOIOIAO 03	5,7	4,43	56,04	1,83		56,23	**4,44**
WCOIOIAO 04	5,7	5,85	97,64			97,97	**5,86**

Table 6: Injuries and censoring

Test Number	Impact Energy (J)	Age (years)	Injury	Censor
PCLE200	6.76	47		right
PCLE201	26.22			right
PCLE202	26.4			right
PCLE203	46.14			right
PCLE204	100.75			right
PCLE205	97.96			right
PCLE206	233.22		Calcaneus fracture	left
PCLE207	7.07	47		right
PCLE215	26.31	56		right
PCLE216	56.06			right
PCLE217	62.28			right
PCLE218	107.12		Calcaneus fracture	left
PCLE219	128.85		Calcaneus fracture	left
PCLE227	40.43	44	Calcaneus fracture	uncensored
PCLE228	104.02		Calcaneus fracture	uncensored
PCLE229	34.31	44	Calcaneus fracture	uncensored
PCLE230	105.34		Calcaneus fracture	uncensored
PCLE249	39.95	64		right
PCLE250	53.99			right
PCLE251	62.26			right
PCLE252	39.94			right
PCLE253	135.72		Calcaneus fracture	left
PCLE254	237.89		Calcaneus fracture	left
PCLE255	40.78	64		right
PCLE256	60.58			right
PCLE257	56.54			right
PCLE258	41			right
PCLE259	134.59		Tibia plafond	right
PCLE260	41.71			right
PCLE261	236.31		Calcaneus fracture	left
PCLE262	41.08	54		right
PCLE263	55.47			right
PCLE264	62.84		Calcaneus fracture	left
PCLE265	40.93			left
PCLE266	41.45	57		right
PCLE267	59.24			right
PCLE268	57.05		Calcaneus fracture	left
WCOIOIAO 01	63.05	49		right
WCOIOIAO 02	103.05		Calcaneus fracture	left
WCOIOIAO 03	56.04	49	Calcaneus fracture	left
WCOIOIAO 04	97.64		Calcaneus fracture	left